**JURNAL SAINS MATERI INDONESIA (JUSAMI)**
ISSN: 1411-1098 (print), 2614-087X (online)
VOL. 26, ISSUE 1 2024
DOI: https://doi.org/10.55981/jsmi.2024.3800

**ORIGINAL ARTICLE**

# Simulation of Mechanical Stress on A Solution-Annealed 15-15Ti Steel using ABAQUS CAE Program

P. Oktavianto[1,2*], A. Purwaningsih[1,3], M.A. Setiawan[1,3], A.H. Handayani[1,4], A.P.A. Mustari[1], and A. Waris[1]

[1]Department of Physic, Institute Technology of Bandung, Jl. Ganesha No. 10, Bandung, Indonesia
[2]Research Center for Nuclear Material and Radioactive Waste Technology – ORTN BRIN, KST BJ Habibie Building 720, Serpong, South Tangerang, Banten, Indonesia
[3]Research Center for Nuclear Reactor Technology - ORTN BRIN, KST BJ Habibie, Serpong, South Tangerang, Banten, Indonesia
[4]Research Center for Radiation Detection and Nuclear Analysis Technology – ORTN BRIN, KST BJ Habibie, Serpong, South Tangerang, Banten, Indonesia

**ABSTRACT** – In addressing the problem of Titanium (Ti) steel (15-15Ti) proposed as the main candidate material for the manufacture of coatings and fuel wrappers for liquid lead-bismuth eutectic (LBE)-cooled fast reactors at high temperatures related to material degradation, such as liquid metal embrittlement (LME) and liquid metal corrosion (LMC). Research related to the creep failure behavior of solution-annealed 15-15Ti steel exposed to LBE at temperatures of 550°C and 600°C using a creep test facility has been conducted. However, in this study, testing the mechanical properties of 15-15Ti steel through tensile testing was not really discussed, even though the mechanical properties of a material are one of the most important things in determining structural design. The mechanical properties obtained from previous research were then simulated using ABAQUS CAE software to determine the stress distribution profile (initial and final) and the mechanical stress-strain performance used to understand more about the 15-15Ti material. The simulation results found that the peak force received by the specimen for a strain rate of 1.1 × 10-5s-1 was 6.0 kN, while for a strain rate of 5 × 10-5s-1, it was 6.2 kN. This means that the specimen used cannot accept a force greater than the peak force value. A stress-strain difference graph was also obtained in the experimental results, with simulation results showing a decrease in the value of the fracture point. This is because the mesh setting in the simulation is not close to a more detailed value.

**ARTICLE HISTORY**
Received: 20 Feb 2024
Revised: 11 Jun 2024
Accepted: 12 Jun 2024
**KEYWORDS**
15-15Ti steel
Tensile test
Mechanical properties
ABAQUS program
Fracture phenomenon

## INTRODUCTION

Generation IV (Gen IV) nuclear reactors promise improved features for an energy resource that is already seen as a reliable and outstanding resource operating at high levels of fuel efficiency, safety, proliferation resistance, sustainability, and cost. Generation IV nuclear reactors have also found material performance and reliability when exposed to higher neutron doses and highly corrosive high-temperature environments. This is because the main consideration for the successful development of generation IV nuclear reactors is the appropriate structural material to use (material selection in nuclear reactors must meet high safety standards, especially in terms of strength and material resistance when exposed to high radiation) [1]. The operating period of Gen IV nuclear reactors, which is 60 years, will require material upgrades over a very long period of time. Stability, high reliability, adequate resources, and easy fabrication, as well as weldability, environmental impact, and aging, are other important aspects that need to be considered during the material selection process [2]. Liquid lead-bismuth eutectic (LBE)-cooled fast reactors are Gen IV nuclear reactors that are inherently safer than liquid sodium-cooled fast reactors due to the chemical inertness of LBE when exposed to air and water. Liquid LBE-cooled fast reactors are also considered a promising technology to address nuclear energy sustainability by closing the fuel cycle and reducing the volume of nuclear waste [3].

A 15 wt% nickel (15-15Ti) is used in the fast reactor owing to its outstanding high-temperature properties, excellent oxidation, and corrosion resistance [4]–[6]. Therefore, 15-15Ti steel has been proposed as the main candidate material for making coatings and fuel wrappers of liquid LBE-cooled fast reactors at high temperatures [7]–[10]. Its mechanical and creep resistance to high temperatures under exposure to large neutrons, as well as its resistance to irradiation-induced swelling, are important properties for such applications [11]–[12]. However, there are challenges regarding material degradation, such as liquid metal embrittlement (LME) and liquid metal corrosion (LMC). The fuel temperature depends on the reactor power; the peak temperature can reach 550°C or even higher. These conditions generate significant hoop stress due to the pressure of the fission gas in the fuel. Under these conditions, the synergy effect of creep and LBE corrosion is a key factor affecting the structural integrity of the fuel rods. LBE corrosion on the specimen surface can promote crack initiation and propagation. Therefore, the creep behavior of 15-15Ti stainless steel interacting with LBE is also an important issue to be addressed, especially at high temperatures [13].

***CORRESPONDING AUTHOR** | A. Nikitasari & R. Riastuti | ✉ waltermellon@batan.go.id

In the study of Gong et al., several creep-to-rupture tests were conducted under constant uniaxial tensile stress conditions (i.e., 300 MPa) to determine the creep failure behavior of solution-annealed 15-15Ti steel exposed to LBE at temperatures of 550°C and 600°C using a creep test facility. From the test results, it was found that at the same temperature, the secondary creep rate of 15-15Ti steel tested in LBE at 500°C was 56 times higher than that tested in air, and at 600°C, it was six times higher. The creep life of 15-15Ti steel exposed to LBE was severely degraded. Creep failure in LBE is dominated by two mechanisms: thermal creep occurring in bulk, causing surface fracture, and mechanisms on the specimen surface associated with uniform dilution corrosion and intergranular cracking. Failure due to intergranular cracking is much faster than that due to uniform surface corrosion. This condition may play an important role in the life limitation of reactor components made of steel [14]. However, in this study, testing the mechanical properties of 15-15Ti steel through tensile testing is not really discussed, even though the mechanical properties of a material are one of the most important things in determining structural design. Tensile tests are conducted to complete basic design information on the strength of a material and as data used to support material specifications [15]. From the tensile test conducted, the values of modulus of elasticity, yield strength, ultimate tensile strength, percent elongation at fracture, percent reduction in area at fracture, modulus of resilience, and toughness (static) can be known so that the mechanical properties of 15-15TI steel are known. Modulus of elasticity is used to determine how elastic material is [16], yield strength to determine the resistance of a material to plastic deformation [17], ultimate tensile strength to determine the maximum nominal stress that a material can withstand before fracture [18], percent elongation at fracture to determine the percentage of length increase achieved by the material before breaking [19], the percent reduction in area at fracture to determine the percentage reduction in tensile cross-sectional area of the specimen at fracture [20], modulus of resilience to determine the amount of energy per unit volume required to cause damage and permanent changes in composition and structure in the sample, and toughness (static) to determine the amount of energy per unit volume required to break the sample completely [21]. However, the mechanical properties data obtained from experiments do not provide data on the distribution of stress that occurs during the tensile test process.

Experiments conducted only provide qualitative data. Qualitative data cannot display the stress profile in detail, so in this paper, the tensile test is simulated using ABAQUS CAE software to determine the stress distribution profile (initial and final) and the stress-strain mechanical performance used to understand more about the 15-15Ti material. ABAQUS CAE is a software that has the ability to model various problems in structural, geotechnical, and other fields in 1D, 2D, and 3D views [22]. The program has an extensive list of material models that can simulate the behavior of some of the most engineering materials, including metals, rubber, polymers, composites, reinforced concrete, flexible and strong foams, and geotechnical materials such as soil and rock [23]. Like many computer programs on the market, ABAQUS software includes computer aided desain/computer aided manufacturing/computer aided engineering (CAD/CAM/CAE), which functions as a program for elastic and plastic analysis. The advantage of ABAQUS over other similar programs is its comprehensive menu of modules. In addition, material testing can be performed by manually entering material data into the input file. The development of the programming language in ABAQUS makes it easier for designers to determine the method used to perform the simulation and analysis processes. The possibility of failures and errors that occur during the running process of input files that have been entered is usually caused by errors in inputting data in the ABAQUS CAE module [24]. ABAQUS can also provide a variety of conveniences for the simulation of linear and non-linear applications. ABAQUS can model multiple element sections with various element section geometries with appropriate model materials and can specify the interaction of each element. In non-linear analyses, ABAQUS can select accurate load summation values and convergence tolerances and continuously adjust them during the analysis process to prove that accurate and efficient solutions are obtained during analysis [23],[25]. ABAQUS was used in this study because of its various advantages, especially in determining the stress distribution profile and mechanical stress-strain. By simulating with ABAQUS, it is hoped that it can be known from the mechanical properties of things that cause creep failure in 15-15Ti steel.

## EXPERIMENTAL METHOD

### Materials and Instruments

The material composition of solution-annealed 15-15Ti steel is presented in Table 1. Table 2 displays the tensile properties of the 15-15Ti alloy. To perform simulations with ABAQUS, the material properties of solution-annealed 15-15Ti steel were obtained from previous research conducted by Gong et al. [10]. In Gong's study, 15-15Ti solution-annealed steel specimens were tested in Ar+5%H2 and air, with temperatures of 550°C and 600°C, and two different strains of $5 \times 10^{-5}$ $s^{-1}$ and $1.1 \times 10^{-5}$ $s^{-1}$. In this study, data from 15-15Ti solution-annealed steel tested in air at 600°C with different strain rates will be used. The tensile test results of both specimens obtained stress-strain curves for each strain rate in Figure 1 and Figure 2.

**Table 1.** Chemical composition of the solution-annealed 15-15Ti steel (wt%) [10]

| C | Cr | Ni | Mn | Mo | Si | Ti | Al | B | P | V | S | Fe |
|---|---|---|---|---|---|---|---|---|---|---|---|---|
| 0.0715 | 16.01 | 16.11 | 1.74 | 1.18 | 0.54 | 0.41 | <0.005 | <0.005 | <0.005 | <0.005 | 0.005 | Bal. |

**Table 2.** The tensile properties of 15-15Ti alloy [26]

| Specimen | Grain Size (µm) | Ultimate Tension Strength (Mpa) | Yield Strength (Mpa) | Total Elongation (%) |
|---|---|---|---|---|
| REC | 2–4 | 690 | 523 | 50.8 |
| SOL | 52 | 541 | 237 | 71.5 |
| ROL | 22–46 | 656 | 406 | 47.1 |
| 15-15Ti (3.67 alloy) | 20–43 | 635 | 325 | 48.0 |

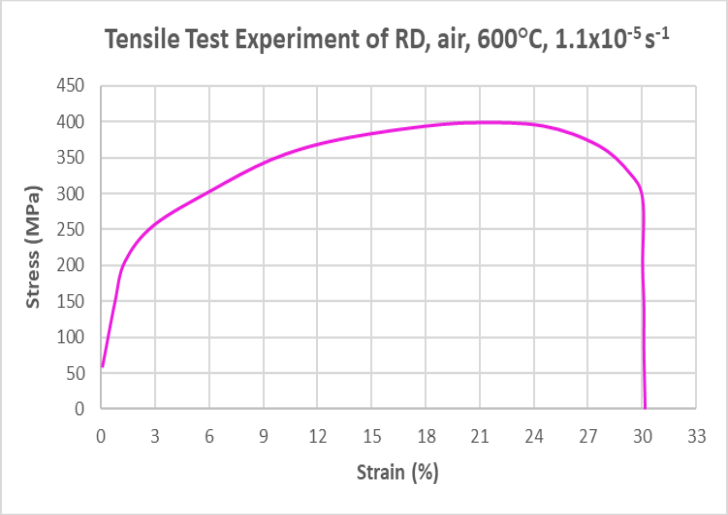


**Figure 1.** Tensile test experiment of solution-annealed 15-15Ti steel in air, 600°C, $1.1\times10^{-5}$ $s^{-1}$

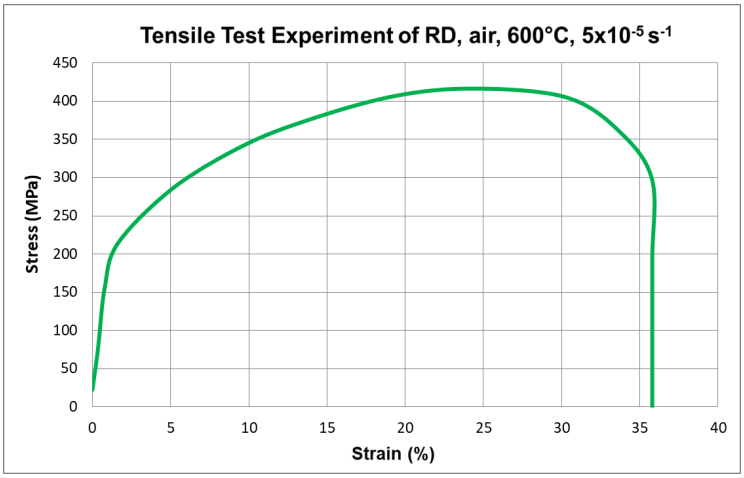


**Figure 2.** Tensile test experiment of solution-annealed 15-15Ti steel in air, 600°C, $5\times10^{-5}$ $s^{-1}$

## Method and Procedure

The facilities available in the ABAQUS CAE program are very complete. Therefore, modeling the specimen directly can be done without using other software. The following steps are to simulate the specimen using the ABAQUS CAE facility.

### Model Geometry

The simulation was conducted using ABAQUS CAE Learning Edition 2023 software. Depending on the user, multiple methods can be used to model the test specimen to be tested. The test specimen model can be drawn directly in ABAQUS CAE or with the help of other programs that have computer aided engineering (CAE) facilities. ABAQUS CAE, which is used as a place to input data into the file, plays an important role for designers who want to do numerical analysis using ABAQUS CAE software. Before starting to draw the model to be made, the first thing to do is prepare the dimensional data of the test object model to be drawn [24]. Based on research data conducted by Gong et al., the

specimen is a solid cylinder with a diameter of 50 mm at the center and 430 mm at both ends. The specimen used for simulation has the dimensions shown in Figure 3. The material composition of 15-15Ti austenitic steel consists of 15% chromium, 15% nickel, and titanium as a modifier. Figure 4 is an image of the test specimen model in ABAQUS with the size corresponding to the size in the example drawing, while Figure 5 presents a 3D specimen model using the finite element method (FEM).

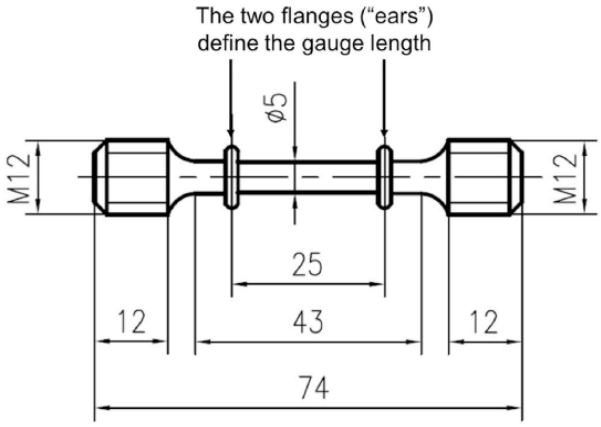


**Figure 3.** Original dimension of specimen

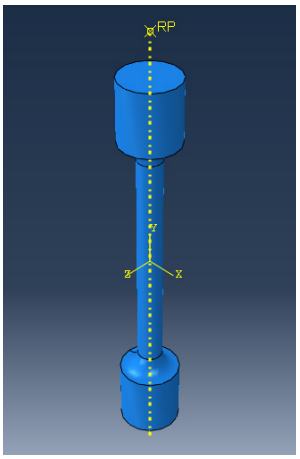


**Figure 4.** Specimen dimensions in ABAQUS

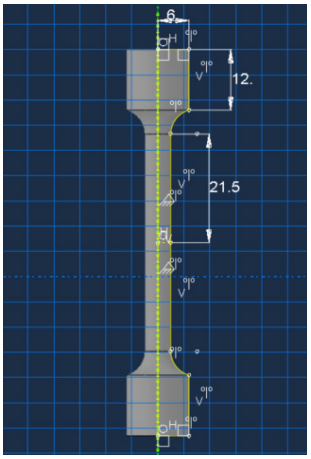


**Figure 5.** 3D model using FEM

### Entering the tensile test input value

Based on the stress-strain curves in Figure 1 and Figure 2, the input values required for the input of mechanical properties in the tensile test used in ABAQUS are obtained. Table 3 shows the input values for the tensile test.

**Table 3.** Tensile test material properties for input data in ABAQUS

| Material | Properties | | | | | | | |
|---|---|---|---|---|---|---|---|---|
| | Mass Density | Elastic | | Plastic | | Ductile Damage | | |
| | | Modulus of Elasticity | Poisson's Ratio | Yield Stress | Plastic Strain | Fracture Stress | Stress Triaxiality | Strain Rate |
| Solution-annealed 15-15Ti steel tested in Air 600°C, $1{,}1\times10^{-5}s^{-1}$ | 7.93E-09 | 196000 | 0.28 | 255.91<br>304.30<br>347.31<br>373.12<br>391.4<br>398.92 | 0<br>0.06<br>0.09<br>0.13<br>0.17<br>0.21 | 0.3 | 0.45 | $1.1\times10^{-5}$ |
| Solution-annealed 15-15Ti steel tested in Air 600°C, $5\times10^{-5}s^{-1}$ | 7.93E-09 | 198978 | 0.28 | 284.70<br>337.64<br>371.76<br>405.88<br>416.47 | 0<br>0.09<br>0.13<br>0.19<br>0.24 | 0.35 | 0.48 | $5\times10^{-5}$ |

The modulus of elasticity is of potential importance in calculating component design, either through analytical equations or through the FEM [27]. The elastic behavior of the reinforcement is defined by this modulus of elasticity value and the poison ratio [28]. The triaxial stress values were obtained from research data conducted by Jan Peirs et al. [29] based on fracture strain values obtained from stress-strain curves, while Poisson's ratio was based on data from Dieter's book [30].

**Setting the step**

ABAQUS has two measures of time in the simulation. One is the total time, which increases across steps, and is the accumulation of the total step time of each common step. Each step also has its time scale (known as step time), which starts at zero for each step. Time-varying loads and boundary conditions can be specified in terms of the time scale [31]. In this simulation, the step is set with the region being the whole model, the type being factor, the interval being the beginning of the step, the factor being 1000, and the target time increment being none.

**Determining load and boundary conditions**

After determining the steps at which the load and boundary conditions (BC) become active, the load and BC conditions must be determined. Three boundary conditions were created, namely:

- The first BC (BC1) restricts the tensile bottom end of the specimen in X, Y, and Z directions, which should be applied during the initial step with the type "Symmetry/Antisymmetry/Encastre." In this BC1, a boundary condition is created with a mechanical category of type Encastre (U1 = U2 = U3 = UR1 = UR2 = UR3 = 0).
- The second BC (BC2) places the specimen as a cell and limits the degrees of freedom U1, U3, UR1, UR2, and UR3 and allows the degree of freedom U2, i.e., the load to be applied only in the Y direction as a distributed load.
- For the third BC (BC3), a surface traction load is applied to the top surface of the specimen to establish a distributed tensile load on the top surface of the specimen. The load is applied during the analysis step. In BC3, the degrees of freedom of U1, U2, UR1, UR2, and UR3 will be set to zero, the BC shall be modified, the 2nd degree of freedom (U2) activated, and the distributed force value shall be established. The applied force will be a stress applied to the surface. The load and boundary condition results are shown in Figure 6.

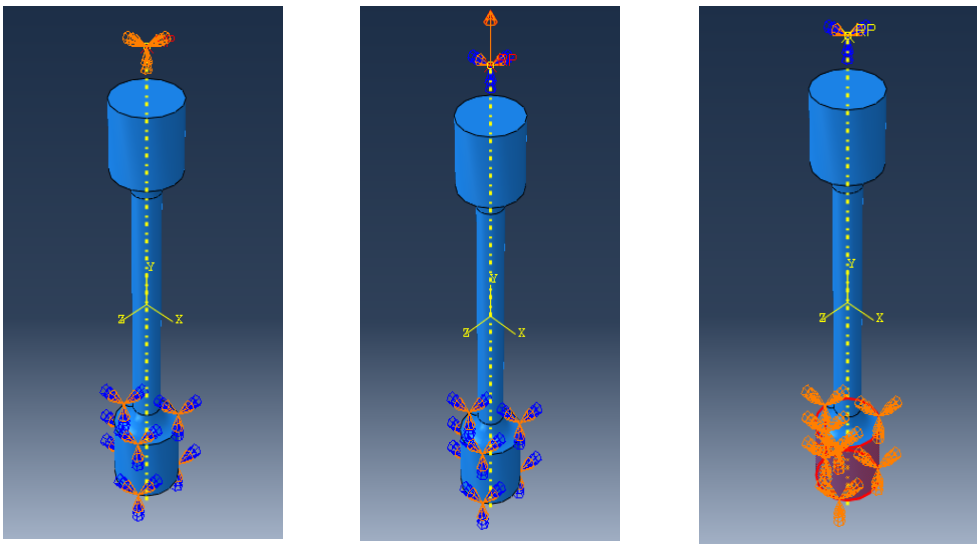

(a) (b) (c)

**Figure 6.** Defining boundary condition: (a) BC1, (b) BC2, and (c) BC3

**Determining the mesh**

In the mesh selection step, the specimen is divided by size 3, with a total number of elements of about 624. The selected mesh is quad-shaped, as shown in Figure 7.

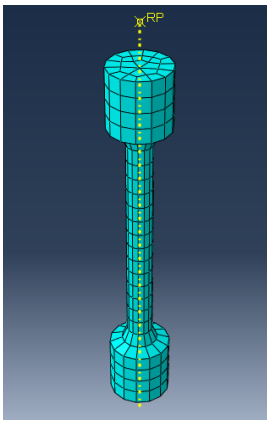


**Figure 7.** Quad shape mesh

## RESULT AND DISCUSSION

### Simulation Result

After all the processes are done, the job that has been done is submitted for analysis (the progress can be monitored from submitted to running to completed). If there are no errors in the previous step, the submitted job will be completed, and the output in the form of a visualization module can be displayed. The results of the tensile test on the rolling direction (RD) specimen tested in the air with a strain rate of 1.1×10-5s-1 obtained a visualization module, as shown in Figure 8.

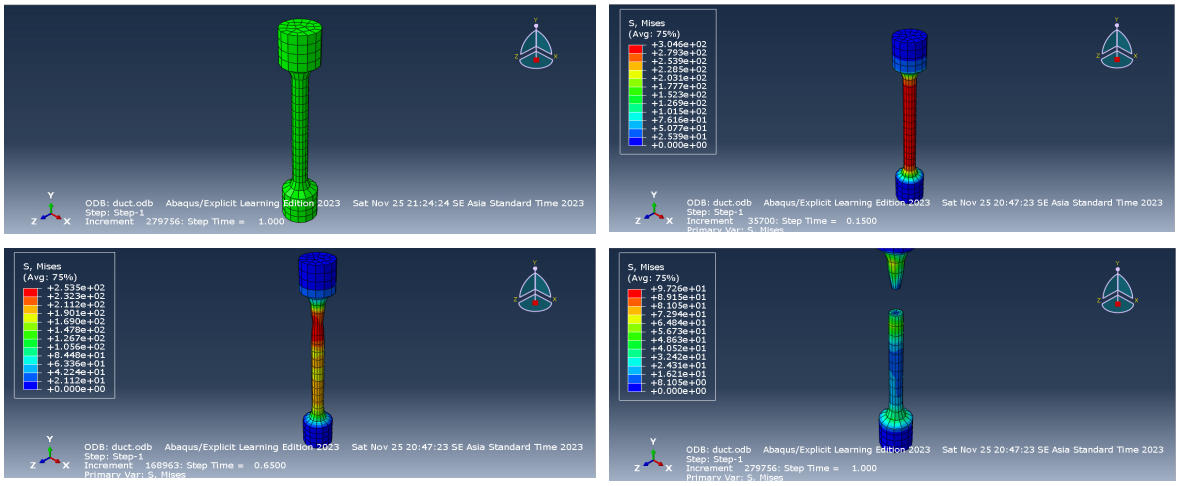


**Figure 8.** Visualization model process with pressure profile of solution-annealed 15-15Ti steel in air, 600°C, $1.1\times10^{-5}$ $s^{-1}$

In Figure 8, it can be seen that the simulation can obtain the stress distribution that occurs. At the beginning of the tensile test, by pulling up, the stress is still evenly distributed along the middle of the specimen, marked in red in the visualization module. The more it is pulled up, the greater the stress at the top than in the other parts, so that over time, the specimen will break at the top. The maximum stress that can be accepted by the specimen is 304.6 MPa. Based on research conducted by Gong et al., experimental results were carried out up to 300 MPa [10]. When compared with the results of the simulation, it can be concluded that in the experiment, the specimen has broken. In another study conducted by Strafella et al., who also tested the creep behavior of 15-15Ti (Si) austenitic steel at 550°C, the specimen was able to withstand stress up to 560 MPa. From the research conducted, the results obtained show that the longer the test time, the greater the creep strain value [11], [32]. In another study conducted by Xu et al., it was shown that the stress peak (maximum stress) at 20°C was greater than at 550°C [33]. After that, the specimen will experience fatigue and become broken. The curve of the relationship between force and displacement is shown in Figure 9. In the curve, it can be seen that the peak force received by the specimen is 6.0 kN (in experiments, the peak force was 5.9 kN).

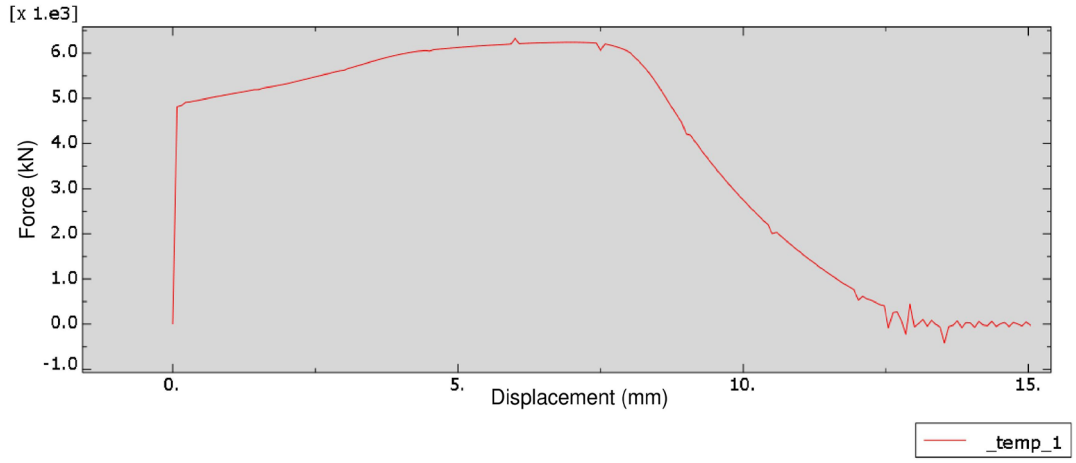


**Figure 9.** Force vs. displacement curve in the visualization module of solution-annealed 15-15Ti steel in air, 600°C, $1.1\times10^{-5}$ $s^{-1}$

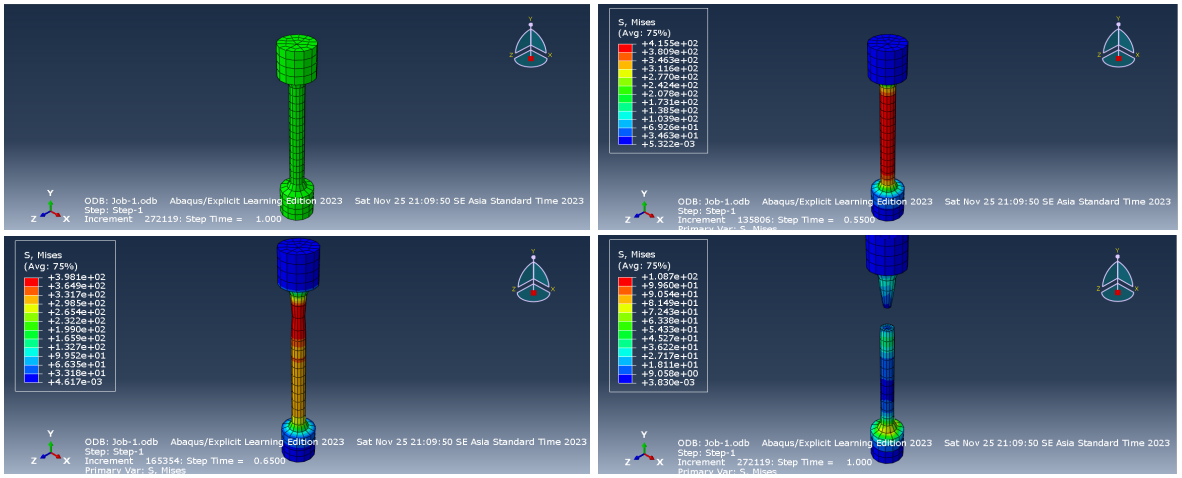


**Figure 10.** Visualization model process with pressure profile of solution-annealed 15-15Ti steel in air, 600°C, $5\times10^{-5}$ $s^{-1}$

We can see in Figure 10 that at the beginning of the tensile test, by pulling up, the stress is the same as the previous specimen, which is still evenly distributed along the middle of the specimen marked in red in the visualization module. The more it is pulled up, the greater the stress at the top than in the other parts, so that over time, the specimen will break at the top. The maximum stress that can be accepted by the specimen is 415.5 MPa. The maximum stress obtained is greater than the previous specimen due to the difference in strain values. Just like before, the research of Gong et al. was conducted experimentally up to 300 MPa (10). When compared with the results in the simulation, it can be concluded that in the experiment, the specimen has not been disconnected. The greater the strain value, the greater the creep strength of the object. After that, the specimen will experience fatigue and become broken. The curve of the relationship between force and displacement is shown in Figure 11. In the curve, it can be seen that the peak force received by the specimen is 6.2 kN (in experiments, the peak force was 5.9 kN).

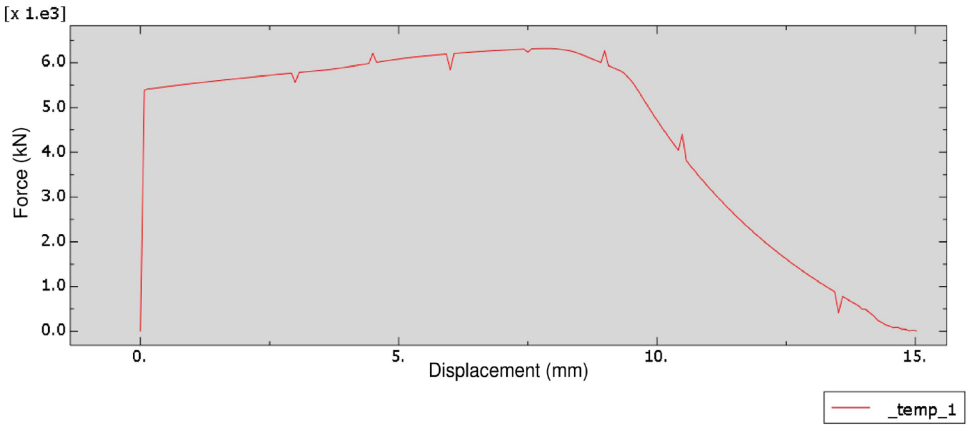


**Figure 11.** Force vs. displacement curve in the visualization module of solution-annealed 15-15Ti steel in air, 600°C, $1.1\times10^{-5}$ $s^{-1}$

Then, the stress-strain curves of the experimental results were compared with the simulation results, as shown in Figure 12 and Figure 13.

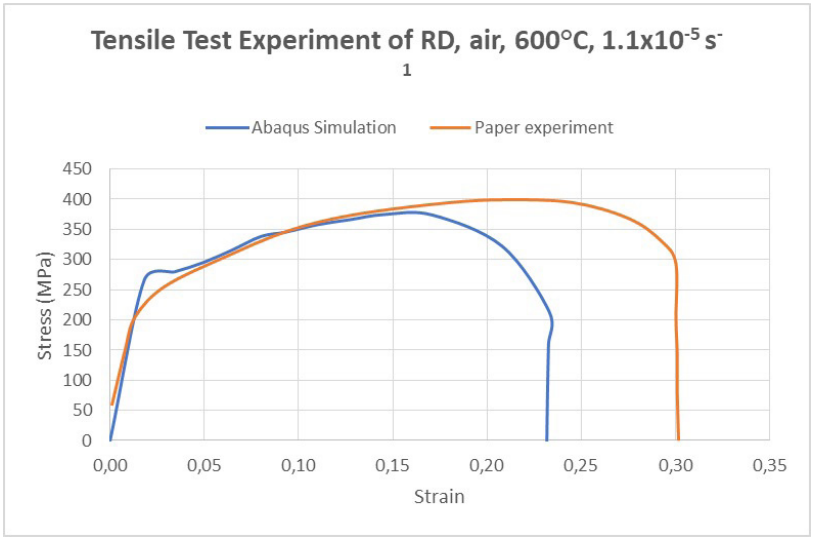


**Figure 12.** Stress vs. strain curves in the visualization module of solution-annealed 15-15Ti steel in air, 600°C, $1.1\times10^{-5}$ $s^{-1}$ from experimental and simulation results

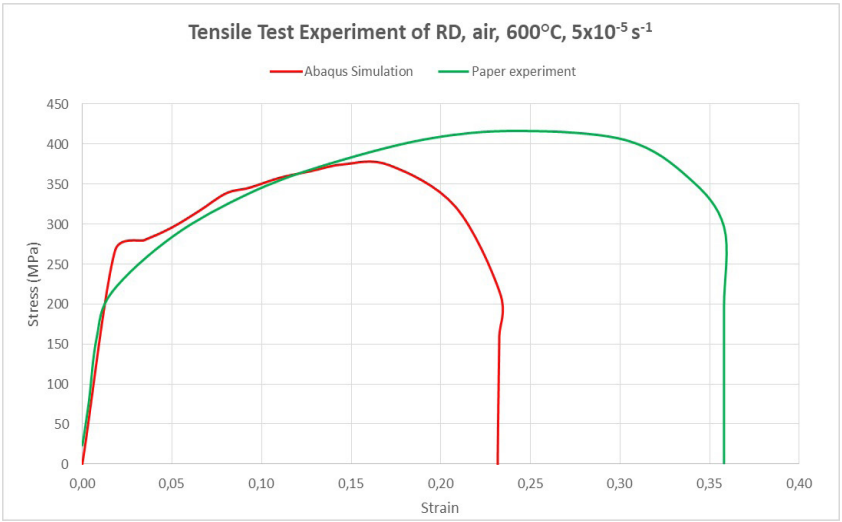


**Figure 13.** Stress vs. strain curves in the visualization module of solution-annealed 15-15Ti steel in air, 600°C, $5\times10^{-5}$ $s^{-1}$ from experimental and simulation results

Figure 12 and Figure 13 show that the simulated stress-strain curve, formed based on data from the experimental stress-strain curve, has shifted in value. Where the fracture point value drops. This could be due to the mesh setting using size 3. The smaller the mesh size, the better and more detailed the analysis. However, because the ABAQUS program used has a node limitation on its mesh settings, the maximum size used is 3. However, by simulating using the ABAQUS program, the stress distribution profile (initial and final) can be known so that the order of breakage of the specimens used is known and the stress-strain mechanical performance of the 15-15Ti material is known so that the stress mechanical analysis can be more detailed. However, there are still many shortcomings in using ABAQUS, such as the limitations of the mesh used. For further research, a more complete ABAQUS program is used so that the analysis obtained can be more detailed.

## CONCLUSION

From the simulation results of tensile tests on solution-annealed 15-15Ti steel specimens with strain rates of $1.1\times10^{-5}s^{-1}$ and $5\times10^{-5}s^{-1}$, it is known that the stress-strain curve data in Gong's research is correct. Validation using the Abaqus simulation showed that the specimen was broken after the tensile test. By using Abaqus simulation, the phenomenon of specimen fracture in sequence from the beginning of pulling and the distribution of stress in the specimen is known, so the location of the fracture position is known, as well as other mechanical phenomena that occur in the specimen. From the simulation, it is found that the peak force received by the specimen for a strain rate of $1.1\times10^{-5}s^{-1}$ is 6.0 kN, while for a strain rate of $5\times10^{-5}s^{-1}$ is 6.2 kN. This means that the specimen used cannot accept a force greater than the peak force value. A graph of the stress-strain difference between the experimental results and the simulation results showing a decrease in the value of the fracture point has also been obtained. This is due to the mesh setting in the simulation not approaching a more detailed value. Simulating using the ABAQUS program, the stress distribution profile (initial and final) can be known so that the order of breakage of the specimens used is known and the stress-strain mechanical performance of the 15-15Ti material is known so that the stress mechanical analysis can be more detailed

## REFERENCES

P. Yvon. *Structural Materials for Generation IV Nuclear Reactors*. Woodhead Publishing, 2016.

L. Chengliang and Y. Mengjia. "The challenge of nuclear reactor structural materials for Generation IV nuclear energy systems." *Nucl Energy SMiRT 20*, 2009.

C. Fazio, V. P. Sobolev, A. Aerts, S. Gavrilov, K. Lambrinou, P. Schuurmans et al. "Handbook on lead-bismuth eutectic alloy and lead properties, materials compatibility, thermal-hydraulics and technologies." *Nucl. Sci.*, pp. 647–730, 2015.

L. K. Mansur, A. F. Rowcliffe, R. K. Nanstad, S. J. Zinkle, W. R. Corwin, and R. E. Stoller. "Materials needs for fusion, Generation IV fission reactors and spallation neutron sources-Similarities and differences." *J. Nucl. Mater.*, vol. 329–333, no. PART A, pp. 166–172.

K. L. Murty and I. Charit I. "Structural materials for Gen-IV nuclear reactors: Challenges and opportunities." *J. Nucl. Mater.*, vol. 383, no. 1–2, pp. 189–195, 2008.

Y. Zhuang, X. Zhang, X. Zhang, T. Peng, H. Fan, X. Zeng, and Q. Yan. "Microstructure and high temperature mechanical properties of the new cladding steel of 15Cr-15Ni-Ti-Y." *Nucl. Mater. Energy*, vol. 31, p. 101200, 2022.

V. Tsisar, C. Schroer, O. Wedemeyer, A. Skrypnik, and J. Konys. "Corrosion behavior of austenitic steels 1.4970, 316L and 1.4571 in flowing LBE at 450 and 550°C with $10^{-7}$ mass% dissolved oxygen." *J. Nucl. Mater.*, 454, no. 1–3, pp. 332–342, 2014.

V. Tsisar, C. Schroer, O. Wedemeyer, A. Skrypnik, and J. Konys. "Long-term corrosion of austenitic steels in flowing LBE at 400° and $10^{-7}$ mass% dissolved oxygen in comparison with 450 and 550°C." *J. Nucl. Mater*., vol. 468, pp. 305–312, 2016.

E. Charalampopoulou, R. Delville, M. Verwerft, K. Lambrinou, and D. Schryvers. "Transmission electron microscopy study of complex oxide scales on DIN 1.4970 steel exposed to liquid Pb-Bi eutectic." *Corros. Sci.*, vol. 147, pp. 22–31, 2019.

X. Gong, Z. Yang, Y. Deng, J. Xiao, H. Wang, Z. Yu, and Y. Yin. "Creep failure of a solution-annealed 15-15Ti steel exposed to stagnant lead-bismuth eutectic at 550 and 600 °C." *Mater. Sci. Eng. A*., vol. 798, p. 140230, 2020.

A. Strafella, A. Coglitore, and E. Salernitano. "Creep behaviour of 15-15Ti(Si) austenitic steel in air and in liquid lead at 550°C." *Procedia Struct. Integr.*, vol 3, pp. 484–497, 2017.

N. Cautaerts, R. Delville, W. Dietz, and M. Verwerft. "Thermal creep properties of Ti-stabilized DIN 1.4970 (15-15Ti) austenitic stainless steel pressurized cladding tubes." *J. Nucl. Mater*., vol. 493, pp. 154–167, 2017.

L. Li, C.-Q. Li, and M. Mahmoodian. "Effect of applied stress on corrosion and mechanical properties of mild steel." *J. Mater. Civ. Eng.*, vol. 31, no. 2, p. 04018375, 2019.

X. Gong, R. Li, M. Sun, Q. Ren, T. Liu, and M. P. Short. "Opportunities for the LWR ATF materials development program to contribute to the LBE-cooled ADS materials qualification program." *J. Nucl. Mater.*, vol. 482, no. 218–228, 2016.

A. Setiawan. "Stress-strain response material polymer poly lactid acid dengan experimental measurements dan numerical simulations."

*J. Tek. Elektron. Engine.*, vol. 6, no. 1, pp. 10–16, 2020.

Instron. *Modulus of Elasticity* [Online]. Available: https://www.instron.com/en/resources/glossary/modulus-of-elasticity

B. Bakri and S. Chandrabakty. "Efek waktu perlakuan panas temper terhadap kekuatan tarik dan ketangguhan impak baja komersial." *J SMARTek*, vol. 4, no. 2, pp. 97–107, 2006.

I. K. Rimpung and I. G. O Pujihadi. "Analisis perubahan kekuatan tarik baja (St. 42) dengan perlakuan panas 800°C." *J. Log.*, vol. 17, no. 2, 2017.

S. Chambers. (2020, June 9). *Elongation : What Is It and Why Does It Matter?* [Online]. Available: https://www.strouse.com/blog/what-is-elongation

E. D'angelo. "Stress-strain relationships during uniform and nona uniform expansion of isolated lungs." *Respir. Physiol.*, vol. 23, no. 1, pp. 87–107, 1975.

C. Y. Lin and J.-H. Kang. "Mechanical properties of compact bone defined by the stress-strain curve measured using uniaxial tensile test: A concise review and practical guide." *Materials (Basel)*, vol. 14, no. 15, 2021.

Muslikh, M. Iman, A. F. Setiawan. *Pemodelan Elemen hingga Struktur Menggunakan ABAQUS*. Yogyakarta: Penerbit Beta Offset, 2020, pp. 8–9.

D. M. T. D. Herlina. "Analisis Balok Beton Berulang Menggunakan Program ABAQUS CAE V6.14 pada Gedung Hotel *IBIS STYLE* dalam Wilayah Gempa III." Bachelor thesis, Universitas Negeri Semarang, Indonesia, 2019.

Azhar. "Analyzing the tensile strength of AISI 1045 coil springs in Avanza 2020 cars : A comparative study of experimental results using simulation technology." *J. Eng. Sci.*, vol. 1, no. 2, pp. 56–71, 2022.

R. N. Arini and R. Pradana. "Analisa tegangan regangan pada balok dengan menggunakan software ABAQUS CAE V6.14." *J. Artesis*, vol. 1, no. 2, pp. 193–198, 2021.

Y. Zhuang, X. Zhang, T. Peng, H. Fan, X. Zhang, Q. Yan, and A. A. Volinsky. "Effects of yttrium oxides on the microstructure and mechanical properties of 15-15Ti ODS alloy fabricated by casting." *Mater. Charact.*, vol. 162, p. 110228, 2020.

D. I. Sakti, B. Setiyana, and M. Tauviqirrahman. "Studi perbandingan investigasi modulus elastisitas antara metode uji tarik dengan metode indentasi pada material styrene butadiene rubber 25 (SBR-25)." *J. Tek. Mesin*, vol. 11, no. 2, pp. 147–156, 2023.

M. A. Rofiq, H. Alrasyid, D. Iranata, and D. Irawan. "Prediksi perilaku lentur kolom beton bertulang mutu tinggi terhadap kombinasi beban perpindahan monotonik dan aksial rendah." *J. Apl. Tek. Sipil*, vol. 16, no. 2, pp. 43–50, 2019.

J. Peirs, P. Verleysen, and J. Degrieck. "Experimental study of the influence of strain rate on fracture of Ti6Al4V." *Procedia Eng.*, vol. 10, pp. 2336–2341, 2011.

G. E. Dieter. *Mechanical Metallurgy*. McGRAW-HILL BOOK COMPANY; 1961.

A. D. Gudayu, L. Steuernagel, and D. Meiners. "The capability of ABAQUS/CAE to predict the tensile properties of sisal fiber reinforced polyethylene terephthalate composites." *Compos. Adv. Mater*, vol. 31, pp. 1–13.

A. Strafella, A. Coglitore, P. Fabbri, and E. Salernitano. "15-15Ti(Si) austenitic steel: Creep behaviour in hostile environment." *Frattura ed Integrita Strutturale*, vol. 42, pp. 352–365, 2017.

J. Xu, J. Chen, X. Zhai, L. Luo, Q. Wu, and Y. Song. "Low cycle fatigue behaviour of 15-15Ti at 20 and 550 ° C under vacuum." *Mater. Sci. Technol.*, vol. 35, no. 9, pp. 1088–1094.

Copyright © 2024 Author(s). Publish by BRIN Publishing. This article is open access article distributed under the terms and conditions of the Creative Commons Attribution-ShareAlike 4.0 International License (CC BY-SA 4.0)